Ti^{3+} on Nb site: A paramagnetic Jahn-Teller center in vacuum-reduced $LiNbO_3$:Mg:Ti single crystals

G. Corradi*
Crystal Physics Laboratory, Institute for Solid State Physics and Optics of the Hungarian Academy of Sciences, P.O. Box 49, Budapest, H-1525 Hungary

I. M. Zaritskii†
Institute of Semiconductor Physics, Ukrainian National Academy of Sciences, 252650 Kiev, Ukraine

A. Hofstaetter
I. Physikalisches Institut, Universität Giessen, D-35392 Giessen, Germany

K. Polgár
Crystal Physics Laboratory, Institute for Solid State Physics and Optics of the Hungarian Academy of Sciences, P.O. Box 49, Budapest, H-1525 Hungary

L. G. Rakitina
Institute of Semiconductor Physics, Ukrainian National Academy of Sciences, 252650 Kiev, Ukraine
(Received 20 April 1998)

An axial EPR signal observed in vacuum annealed $LiNbO_3$ single crystals doped with 8 mol % Mg and 0.05 mol % Ti has been attributed to Ti^{3+} on Nb site. The **g** tensor components ($g_{\parallel}=1.760\pm0.005$ and $g_{\perp}=1.786\pm0.005$ for $T=5$ K and $g_{\parallel}=g_{\perp}=1.893\pm0.005$ for $T=74$ K), resulting in outstandingly low values of the orbital reduction factor (from $k=0.16$ to 0.13), can be explained by a dynamic pseudo-Jahn-Teller effect. The vibronic coupling of the center is much stronger than that reported for other nd^1 centers with similar trigonally distorted octahedral coordination in $LiNbO_3$ like the Ti^{3+} on Li site and trapped Nb^{4+} polarons on both cation sites. Stronger coupling for ions on or near the Nb site is understood as a result of smaller trigonal splitting of the ground state due to the more central position of the Nb site in the oxygen octahedron. Electron transfer from the observed Ti^{3+} center to lattice niobiums, resulting in Nb^{4+} trapped polarons, has been stimulated by illumination in the near UV region. The average energy difference of the involved $Ti^{4+/3+}$ and $Nb^{5+/4+}$ donor levels has been estimated to be 70 ± 23 meV depending also on the distance of compensating Mg^{2+} ions on nearby Li sites. [S0163-1829(98)04534-2]

I. INTRODUCTION

Titanium is a standard dopant used for waveguide production in $LiNbO_3$ that is just one of the countless applications of this ferroelectric material well known in optoelectronics, nonlinear optics, holography, and acoustics. The Ti^{3+} ions ($3d^1$ configuration), obtained by recharging the initially present Ti^{4+} ions, can be incorporated at cation sites inside oxygen cages of trigonally distorted octahedral symmetry. The splitting of their Γ_5 ($^2T_{2g}$) ground-state multiplet is expected to result in a nearly degenerate ground-state subject to a possible pseudo-Jahn-Teller (JT) effect. The same is expected also for Nb^{4+} centers ($4d^1$ configuration) obtained by recharging the pentavalent niobiums in the crystal.

Such an effect was, in fact, observed for Ti^{3+} substituting for Li^+ in $LiNbO_3$, and was manifested as a decrease of the orbital reduction factor k in EPR.[1,2] A value of 0.58 has been observed instead of k values between 0.7–0.8 valid for non-JT $3d$ ions in Al_2O_3, which is a moderately covalent crystal essentially isostructural with $LiNbO_3$.[3,2]

The EPR parameters reported for Nb^{4+} centers in $LiNbO_3$ strongly depended upon the presence of the Mg dopant.[4–6] It was suggested that in $LiNbO_3$:Mg the rather weak anisotropy of the Nb^{4+} EPR spectrum indicating the quenching of the trigonal crystal field[5] and the observed tetragonal deformation of the recharged NbO_6 complex[6] might be due to a Jahn-Teller effect. The corresponding effects were much weaker in the absence of the Mg dopant.[7,1]

Magnesium (which is another standard dopant of $LiNbO_3$ used as a rule in concentrations slightly above a threshold of 5–6 mol % to reduce optical damage in laser applications) is known to eliminate as-grown antisite Nb_{Li}^{5+} defects[8] (the lower index indicating the substitution site). Accordingly, in $LiNbO_3$:Mg the electron irradiation[4] or vacuum annealing treatments,[4–6] used for the preparation of the paramagnetic Nb^{4+} state, affect the Nb_{Nb}^{5+} ions of the normal lattice, in contrast to undoped $LiNbO_3$ where only antisite Nb_{Li}^{5+} defects are recharged as a result of the same treatments. Various propositions have been put forward to explain the trapping and stabilization of electrons at normal Nb lattice sites, such as the presence of a substitutional Mg^{2+} ion in the nearest Li coordination sphere[4–6] and a polaron effect.[5] It should be pointed out that the annealing treatments used in these references were somewhat different, which is a pos-

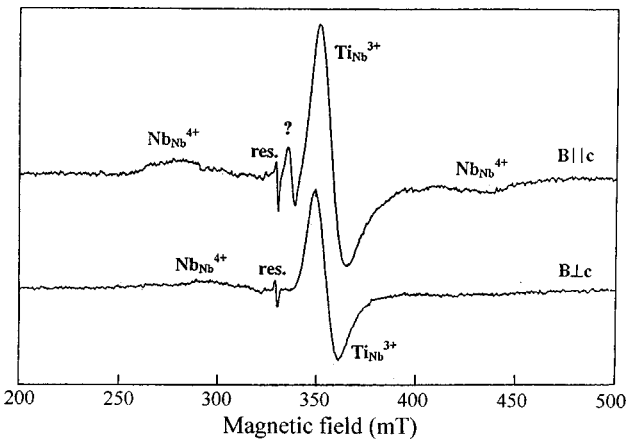

FIG. 1. First derivative EPR spectrum in vacuum annealed $LiNbO_3$:Mg:Ti at $T=14$ K for the magnetic field oriented parallel and perpendicular to the crystal *c* axis. The feature with a question mark is an unidentified signal, possibly Ti_{Li}^{3+}, the signal near $g=2.0$ is due to the resonator. For a detailed description of the hyperfine-broadened Nb_{Nb}^{4+} signal, see Ref. 6.

sible explanation for the slightly different g factors and hyperfine constants obtained for Nb_{Nb}^{4+} centers in these works.

These results served as a clear motivation for us to look for the Ti^{3+} center in overthreshold $LiNbO_3$:Mg crystals, where Ti is expected to substitute for Nb. As in the case of the Nb^{4+} center, such a change in the substitution site should lead, despite the unchanged trigonal point symmetry and the nearly identical octahedral oxygen coordination, to an enhancement of the Jahn-Teller effect. Earlier attempts to prepare the Ti^{3+} state in $LiNbO_3$:Mg:Ti by low-temperature γ irradiation failed,[6] in contrast to the case of $LiNbO_3$:Ti where such a treatment was successful.[9,10] Therefore, in the present work vacuum annealing has been applied, resulting, in fact, in a reduction of the initial Ti^{4+} state. The parameters of the center attributed to Ti_{Nb}^{3+} are compared to those of Ti_{Li}^{3+} and Nb_{Li}^{4+} centers in $LiNbO_3$ and Nb_{Nb}^{4+} centers in $LiNbO_3$:Mg. The possible reason for the enhancement of the Jahn-Teller coupling and the effect of temperature is discussed. We also report on light-induced electron transfer from Ti^{3+} to Nb^{5+} ions, resulting in Ti^{4+} and Nb^{4+} centers.

II. EXPERIMENT

Double-doped $LiNbO_3$ samples have been grown in Budapest from Merck suprapure and Grade I Johnson-Matthey starting materials using a balance-controlled Czochralski method and melts with a congruent Li/Nb ratio containing 8 mol % Mg and 0.05 mol % Ti. Single-doped crystals were also prepared for comparison. The portion of dopants incorporated into the crystals has been investigated by atomic absorption analysis.[11] The distribution coefficient for single doping with Ti was found, in accordance with previous results,[12] to be somewhat smaller than 1, however, the presence of the Mg codopant was seen to increase the built-in amount of Ti by roughly 100%.[11] The concentration of Ti in the double-doped samples used has been estimated to be 0.06 ± 0.02 mol %. Samples of typically $2\times3\times8$ mm^3 size were reduced by annealing during one hour at 920 °C in a vacuum of 5×10^{-5} torr, with subsequent slow cooling to room temperature. As a result of annealing, the originally transparent and colorless samples assumed a slightly smoky tint. Before annealing, the $LiNbO_3$:Mg:Ti samples showed no EPR signals in accordance with earlier measurements.[6]

The EPR measurements in the 4–80 K temperature range have been carried out in the *X* band (~9.25 GHz) using an ESP-300 Bruker spectrometer equipped with an Oxford Instruments helium gas-flow cryogenic system. A 150 W xenon lamp either without filter or together with UV filters having cutoff wavelengths in the 300 to 350 nm region (comparable with the wavelength ~320 nm characterizing the band gap[13]), was used for *in situ* low-temperature illuminations.

III. EXPERIMENTAL RESULTS

The EPR signal recorded in the $LiNbO_3$:Mg:Ti samples after vacuum annealing is shown in Fig. 1 for $T=14$ K and

TABLE I. ESR and Jahn-Teller parameters of Ti^{3+} and Nb^{4+} centers in $LiNbO_3$:Mg (centers on Nb site) and $LiNbO_3$ (centers on Li site). The values of the spin orbit constant $\lambda(Ti^{3+})=123$ cm^{-1} and $\lambda(Nb^{4+})=600$ cm^{-1} are taken from Ref.14. The measurement errors are 0.005 for g values, 0.5 mT for linewidths, and 2 K for temperature.

Center	T K	$g_\parallel$	$g_\perp$	$\Delta B_\parallel$ mT	$\Delta B_\perp$ mT	θ	λ/Δ	Δ cm^{-1}	k	κ_1	W_{JT} cm^{-1}	Ref.
Ti_{Nb}^{3+}	5	1.760	1.786	41	~40	13.7°	0.45	270	0.16	0.21	270	the
	20	1.857	1.860	13.5	12.0	10.3°	0.31	400	0.14	0.19	290	present
	74	1.893	1.893	10.0	12.0	9.2°	0.26	470	0.13	0.17	300	work
Ti_{Li}^{3+}	20	1.961	1.840	3.0	5.2	5.2°	0.14	880	0.58	0.77	45	(1)
	77	1.966	1.862	7.0	13.0	4.7°	0.12	990	0.54	0.72	56	(10)
Nb_{Nb}^{4+}	20	1.85	1.84	10.0	10.0	10.7°	0.32	1865	0.17	0.23	255	(5)
	77	1.87	1.82	11.0	11.0	9.8°	0.28	2100	0.26	0.35	180	(6)
Nb_{Li}^{4+}	20	1.90	1.72	6.0	8.0	7.9°	0.22	2700	0.63	0.84	30	(1) and (7)
	77	1.95	1.79	7.0	14.0	5.5°	0.15	4050	0.70	0.93	12	(10)

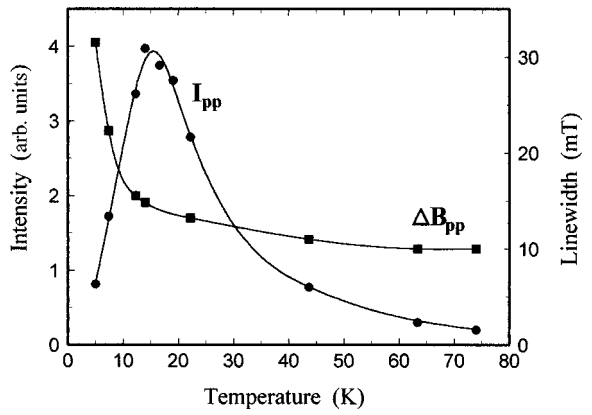

FIG. 2. Temperature dependence of the peak-to-peak intensity and peak-to-peak linewidth of the first derivative EPR signal of the Ti^{3+}_{Nb} center for $\mathbf{B}\|\mathbf{c}$, the lines only serving as guides for the eye.

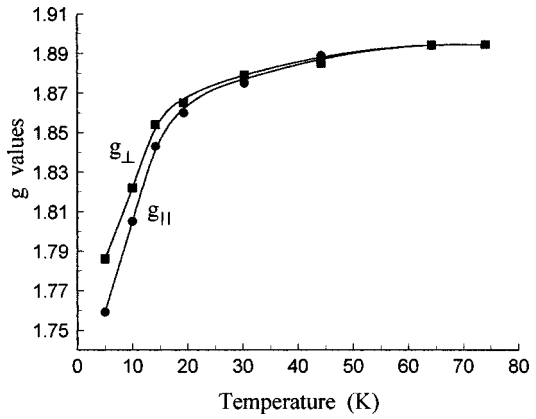

FIG. 3. Temperature dependence of the **g** tensor components of the Ti^{3+}_{Nb} center, the lines only serving as guides for the eye.

two orientations of the magnetic field **B** with respect to the crystal *c* axis. The spectrum is essentially a superposition of a broad, nearly structureless Nb^{4+}_{Nb} signal[6] better visible for $\mathbf{B}\|\mathbf{c}$, and a single-line signal having axial symmetry and a slightly asymmetric line shape, and attributed, for reasons discussed later, to Ti^{3+}_{Nb}. The weak unidentified signal for $\mathbf{B}\|\mathbf{c}$ at $g=1.962$ (peak-to-peak width $\Delta B_{pp}=4$ mT) has parameters comparable to those of the Ti^{3+}_{Li} center observed[1] in $LiNbO_3$:Ti (see Table I). The EPR and other parameters of the Ti^{3+}_{Nb} center derived by using a simple axial $S=\frac{1}{2}$ Zeeman spin-Hamiltonian $\mathcal{H}=\mu_B\mathbf{BgS}$ are shown in Table I, together with those of other nd^1 centers.

A. Temperature dependence of the EPR signal

The temperature dependences of the peak-to-peak intensity I_{pp} and the peak-to-peak width ΔB_{pp} of the first derivative of the EPR signal are shown in Fig. 2. Both have an anomalous character. The signal intensity has a sharp peak at $T=14$ K, and decreases for both higher and lower temperatures. The linewidth shows a monotonous broadening towards lower temperatures, the change becoming rather rapid below 10 K, making the signal practically unobservable for the lowest temperatures. The signal was not saturated for temperatures as low as 5 K up to a microwave power of 0.3 mW. For temperatures above 80 K the signal again becomes too weak to be observed, this time despite narrowing. The temperature dependence of the integral intensity (given by double integration of the first derivative signal) does not follow a Curie law. The deviation is conspicuous for $T>20$ K where the peak-to-peak intensity decreases much sharper than $1/T$ involving a still sharper decrease of the integral intensity due to line narrowing with rising T. A detailed analysis shows that even a Curie-Weiss behavior can be excluded.

The temperature dependence of the **g** tensor components $g_\|$ and $g_\perp$ is shown in Fig. 3. For $T>15$ K the difference between both components is smaller than the measurement error 0.005, i.e., the signal is practically isotropic. It should be pointed out that for $T<15$ K the relation $g_\|<g_\perp$ holds. This situation is very unusual for nd^1 ions with a triplet ground state[1,2,14,7] (see also Table I). The steep critical-like temperature dependence of $g_\|$ and $g_\perp$ in the low-temperature region is another peculiarity of the system.

B. Photoexcitation effects

The optical excitation of the crystal in the near UV at low temperatures (5–30 K) resulted in a ''momentary'' decrease of the Ti^{3+}_{Nb} signal and a simultaneous increase of the Nb^{4+}_{Nb} EPR signal. The spectra are shown in Fig. 4 for $T=14$ K and show a roughly 60% decrease in the numbers of Ti^{3+}_{Nb} centers and a corresponding increase for Nb^{4+}_{Nb}. The Ti^{3+}_{Nb} signal also becomes slightly narrower, e.g., at $T=14$ K the linewidth decreases from 15 to 12.5 mT. These numbers were essentially the same with or without UV filters.

Partial recovery can be observed if the light is switched off, as shown schematically in Fig. 5 for the integral intensities of the signals. Some 18% and 35% of the light-induced change in the Ti^{3+} and Nb^{4+} center numbers, respectively, is recovered. The rest of the changes is stable at temperatures below 30 K but disappears if the sample is heated to higher temperatures. At $T=74$ K, 83% and 112% of the Ti^{3+} and Nb^{4+} center numbers observed before illumination can be seen, respectively, and above 90–120 K recovery is complete. The kinetics of the partial dark recovery process for

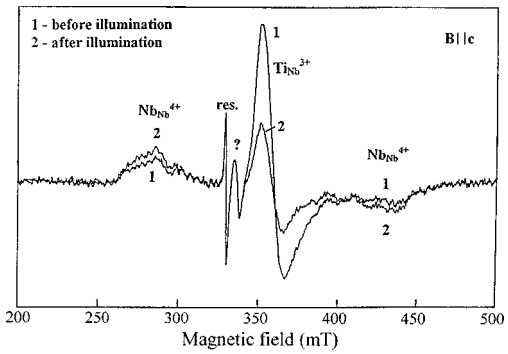

FIG. 4. The effect of illumination on the EPR spectrum at $T=14$ K; for additional features see caption of Fig. 1.

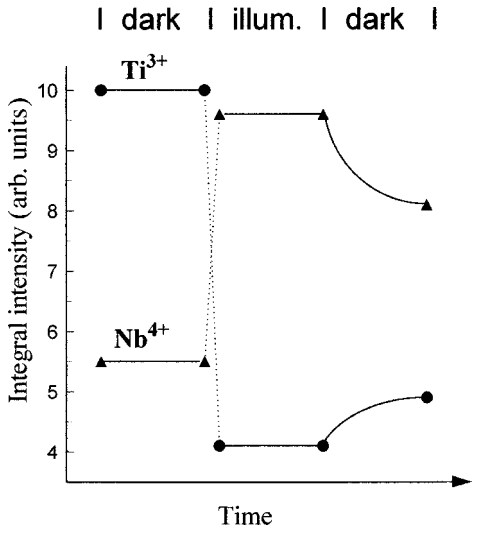

FIG. 5. Schematic representation of integral intensity changes of the Ti^{3+}_{Nb} and Nb^{4+}_{Nb} EPR signals during and after illumination at $T=14$ K.

Ti^{3+} together with its temperature dependence have been investigated in detail for $T=12-30$ K. The results for a given temperature can be described by the exponential approximation

$$\Delta I_{pp}(t) \simeq \Delta I_{pp}(0) e^{-t/\tau}, \tag{1}$$

where ΔI_{pp}(t) is the recoverable part of the light-induced intensity change for time t after switch-off. The values of the time constant τ derived from our experiments are shown in Fig. 6 and can be approximated by the temperature dependence

$$\tau(T) \simeq \tau_0 e^{\Delta E_d / k_B T}, \tag{2}$$

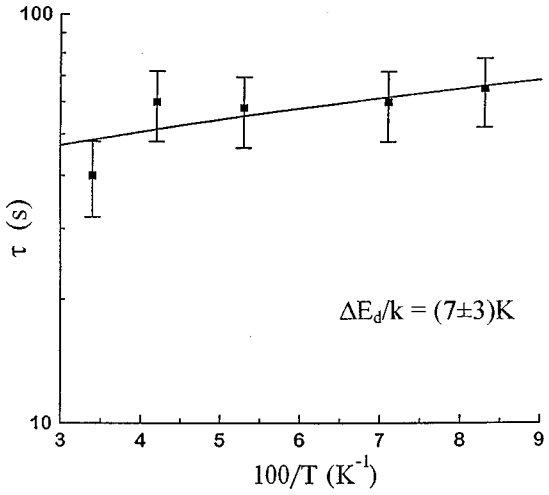

FIG. 6. Arrhenius plot of the time constant characterizing the partial recovery of the Ti^{3+}_{Nb} EPR signal in the dark after illumination.

with the value $\Delta E_d/k_B=(7\pm3)$ K, which can be considered as the activation energy of recovery in the dark. For the parameter τ_0, we obtain the value 40 ± 10 s.

IV. DISCUSSION

The EPR signal observed near $g=1.86$ must be due to titanium, as in similar crystals but doped only with Mg or grown without dopants no such signals could be produced (see also Refs. 6 and 9). The signal is appreciably shifted with respect to Juppe and Schirmer's[1] Ti^{3+} EPR line (which could be reproduced also in our $LiNbO_3$:Ti crystals[9,10]) so there must be a distinct change in Ti incorporation due to the presence of Mg.

In the absence of Mg, the substitution site of Ti could be identified as the Li site if Ti concentrations of 1 mol % or below were used. These results have been obtained by extended x-ray-absorption fine structure,[15] proton induced x-ray emission, or Rutherford backscattering spectroscopy/channeling[16] and perturbed angular correlation methods.[17] For Mg-codoped (over the 5–6 mol % threshold) crystals, an at least partial change of the substitution site from the Li^+ to the Nb^{5+} site has been predicted for dopant cations with larger valences.[18,8] This has been experimentally verified for the Hf dopant[19,20] that is isoelectronic with Ti, and also for Cr^{3+} ions[21–23] and Fe^{3+} ions.[24,25] Therefore, we tentatively attribute the observed EPR signal to Ti^{3+} on the Nb site. This model is supported by our EPR data, especially if the trends for Ti^{3+} and Nb^{4+} ions in $LiNbO_3$ and $LiNbO_3$:Mg, to be discussed in the next section, are taken into account.

We do not think that the signal comes from a perturbed variant of the Ti^{3+}_{Li} center, as the latter is already a perturbed center inevitably having charge compensation in nearby cation spheres (in its stable Ti^{4+}_{Li} charge state the center by itself would have a threefold surplus positive charge). In our opinion, changes in the details of cationic charge compensation would have smaller effects on the center properties. Some indirect support for the Ti^{3+}_{Nb} model comes from a strongly asymmetric EPR signal at similar g values seen in heavily Ti-doped and reduced $LiNbO_3$ waveguide material and tentatively attributed to two unspecified Ti^{3+} centers with overlapping spectra.[8,2] For the large concentrations in question, various substitution sites may be expected including the Nb site as a most straightforward possibility.

A. Discussion and comparison of EPR and Jahn-Teller parameters

Both for Li and Nb substitution the Ti^{3+} ions are incorporated inside octahedral oxygen complexes distorted along the trigonal c axis of the crystal with a site symmetry C_3. Due to the cubic component of the crystal field the orbital quintet D term of the $3d^1$ ground state splits into a lower Γ_5 triplet and a higher Γ_3 doublet with a splitting of 10 Dq. As 10 Dq is of the order of 20 000 cm^{-1}, the doublet excited state has practically no effect on the triplet ground state and only this Γ_5 (T_2) triplet has to be further considered (see Fig. 7). Due to the trigonal component of the crystal field the triplet is split into a singlet Γ_1 ground state and an excited Γ_3 doublet separated by the trigonal splitting Δ. The spin-

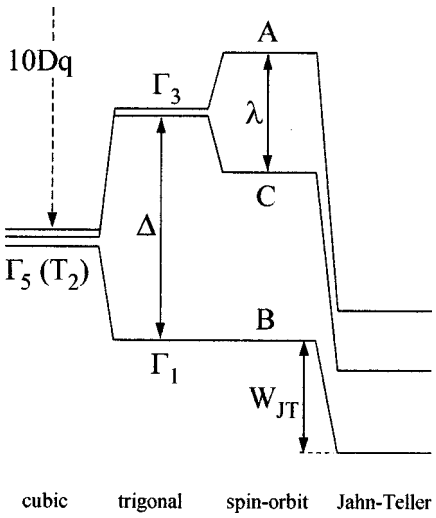

FIG. 7. Splitting of the Γ_5 ($^2T_{2g}$) ground state for an nd^1 ion in trigonally distorted octahedral coordination and first-order Jahn-Teller reduction of the splitting.

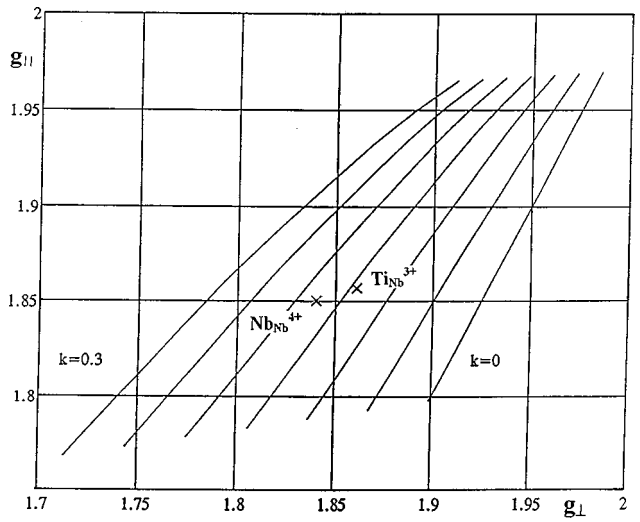

FIG. 8. Parametric plot of the g components for small values of the reduction factor k, calculated using Eq. (4). Experimental values for Ti_{Nb}^{3+} and literature data for Nb_{Nb}^{4+}, both given for $T=20$ K, are indicated by crosses.

orbital coupling splits the excited doublet, which leaves us with three Kramers doublets having the energies (still in the static field approximation without the JT effect):

$$W_A \simeq \Delta + \lambda/2, \quad W_B \simeq 0, \quad W_C \simeq \Delta - \lambda/2, \tag{3}$$

where λ is the spin orbital coupling constant. The **g** tensor components in the ground state B are given by Abragam and Bleaney[14] as

$$g_\parallel = (2+k)\cos 2\theta - k,$$

$$g_\perp = |1 + \cos 2\theta - \sqrt{2}\ k\ \sin 2\theta|, \tag{4}$$

where $\tan 2\theta = \sqrt{2}\ \lambda/(\Delta + \lambda/2)$ and $k = k_{\pi\pi}$ is the factor of orbital reduction due to the formation of covalent π bonds with ligands.

Now, if the experimentally determined g factors in conjunction with Eq. (4) lead to a k value appreciably lower than 0.7–0.8, this has to be considered as a proof for additional vibronic reduction due to a dynamic JT effect.[14,1,2] The values of k derived for the Ti_{Nb}^{3+} center are considerably smaller than those of the related nd^1 ions in $LiNbO_3$ systems (see Table I), and correspond to the range $k \ll 1$ where $g_\parallel < g_\perp$ holds, meaning that the vibronic reduction is exceptionally strong. The extension of the well-known $g_\parallel$ versus $g_\perp$ plot[14,1] for parameter values $k < 0.3$ has been calculated using Eq. (4) and is shown in Fig. 8. Values of θ derived together with those of k can be used for finding the ratio λ/Δ. To proceed towards separate values of λ and Δ, together with Ref. 2, we chose, still in a static non-JT approximation, $\lambda \simeq 0.8\lambda_0 = 123\ \text{cm}^{-1}$ where $\lambda_0 = 154\ \text{cm}^{-1}$ is the free ion value of the Ti^{3+} spin-orbit constant.[14] A similar choice[14] for Nb^{4+} is $\lambda \simeq 0.8\lambda_0 = 600\ \text{cm}^{-1}$.

The solution of the $T \times e$ vibronic problem (taking into account the interaction of the electronic T term with the tetragonal vibrations of the octahedral complex) yields three equilibrium configurations of the complex, each with ground-state energies lowered by W_{JT} (see Fig. 7). In this case the EPR spectra can still be described by Eq. (4), however, the spin-orbit interaction, the trigonal splitting, and the orbital moment have to be reduced by the factor[14]

$$\kappa_1 = e^{-3W_{JT}/2\hbar\omega}, \tag{5}$$

with respect to values received in the static approximation. Here W_{JT} is the JT energy and ω is the frequency of the tetragonal vibrations. This reduction is indicated in Fig. 7 for the parameters λ and Δ. The values of these parameters given in Table I are the ones of the static approximation. For an estimate of W_{JT}, one may use the relation

$$\kappa_1 = k/k_{\pi\pi}, \tag{6}$$

with $k_{\pi\pi} = 0.75$ and $\hbar\omega = 258\ \text{cm}^{-1}$ (see Ref. 2).

The above treatment of the JT effect is a first-order approximation. For Nb^{4+} centers, estimates of the second-order term in the energy expression[14,3,26] are appreciably smaller than the first-order term, but for Ti^{3+} the terms are almost comparable (see also Ref. 2). As the perturbation series proceeds with alternating signs there is a fair chance that our semiempirical first-order estimates included in Table I are qualitatively correct for predicting some trends. A nonperturbative calculation of all interactions relevant for the ground state of Ti^{3+}, including the vibronic coupling of the Γ_1 and Γ_3 states, has been performed by Thiemann *et al.*[2] For the parameter value $\lambda/\Delta = 0.15 \pm 0.2$, valid for the Ti_{Li}^{3+} center, they obtained the JT energy $319 \mp 100\ \text{cm}^{-1}$. This is larger than the estimate for Ti_{Li}^{3+} in Table I, $W_{JT} \simeq 45\ \text{cm}^{-1}$, but is comparable to the estimates for Ti_{Nb}^{3+}. The approach of Ref. 2 is presently limited by a number of simplifying assumptions including the small number (up to two) of JT-active phonons that can be taken into account. Increasing the number of phonons seems to be important for describing a nearly isotropic **g** tensor,[2] which is the case for Ti_{Nb}^{3+}.

For the discussion of data on Ti^{3+} centers, it is useful to also include literature data on related Nb^{4+} centers having well-established substitution sites.[8,5,6,10] Such a comparison

is made in Table I. For Nb_{Nb}^{4+} centers, we included EPR data obtained in $LiNbO_3$:Mg (6 mol % Mg) at the temperatures 20 K (Ref. 5) and 77 K (Ref. 6) neglecting small deviations from axiality. It should be pointed out that data reported for the same center in $LiNbO_3$ single doped with 7.25 mol % Zn or 1.5 mol % In or double-doped with 6.5 mol % Zn and 1.5 mol % In also exhibit strong vibronic coupling[5] fulfilling, in particular, the relation $g_{\parallel} < g_{\perp}$.

Now we proceed by comparing dopant ions and substitution sites. For a given site and temperature the Ti^{3+} centers always have several times smaller trigonal splittings and clearly larger JT energies than the Nb^{4+} centers. This seems to be related to the smaller positive charge of Ti^{3+} resulting in larger ligand distances. Due also to the smaller spin-orbit constant of Ti^{3+}, for the Ti_{Nb}^{3+} center the JT coupling becomes a large and probably even a dominant interaction among those relevant for the ground-state splitting. On the other hand, for a given nd^1 ion the values of the trigonal splitting are significantly smaller for Nb substitution than for Li substitution (see Table I). This holds both in the static approximation (Δ) and in the first-order JT approximation ($\kappa_1 \Delta$). Such a difference is of key interest for the discussion of the JT effect at different sites and originates from the structure of $LiNbO_3$ in its ferroelectric phase (see, e.g., Ref. 8): lattice Nb's are situated closer to the center of their oxygen cage than lattice Li's (the latter being appreciably displaced along the C_3 axis towards three oxygens) a feature at least partly shared by substituents. Consequently, the trigonal component of the crystal field is expected to be weaker for nd^1 ions on the Nb site, resulting in a ground state that is closer to degeneracy, meaning a larger pseudo-JT effect. This is reflected by increased W_{JT} energies and strongly reduced values of k and κ_1 (see Table I). These quantities indicate increasing JT coupling in the order Nb_{Li}^{4+}, Ti_{Li}^{3+}, Nb_{Nb}^{4+}, Ti_{Nb}^{3+}, which is strongly correlated with the net uncompensated charges of these centers $(+3,+2,-1,-2)$. As shown for the $3d^9$ JT ions Ni_{Li}^{+} and Cu_{Li}^{2+} in $LiNbO_3$, a surplus charge may have radical consequences also for the tetragonal deformation of the oxygen octahedron in the JT complex.[27]

It is more difficult to discuss the temperature variations of the parameters in Table I. For all four centers the values of the trigonal splitting Δ show an increase for higher temperature possibly indicating for Nb^{4+} centers a relaxation away from the center of the octahedron (a similar argument for Ti^{3+} centers is less reliable due to stronger vibronic coupling). This Nb^{4+} displacement should be compared with the relaxation of a normal lattice Nb^{5+} ion towards the center of the octahedron while approaching the paraelectric phase, and an opposite behavior for lattice Li^{+} ions.[12,8]

The steeper than Curie-like decrease of the EPR intensity of Ti_{Nb}^{3+} with increasing temperature (see Fig. 2) may be related to a partial thermal depopulation of the ground state. Even without vibronic reduction, the energy difference between the ground and first excited levels $\Delta W = \Delta - \lambda/2$ is rather small. In fact, using the data in Table I for Ti_{Nb}^{3+} at $T = 20$ K one has $\Delta W = 339\ \mathrm{cm}^{-1}$. If there is a substantial additional vibronic reduction for ΔW, the excited state becomes thermally accessible. (Note that the excited state yields no EPR absorption in the $g = 2$ region.[14]) In this case, however, one should also have an Orbach-type broadening that is not observed below 74 K. In the comparable case of Ti^{3+} in yttrium aluminoborate, where Ti^{3+} occupies a octahedrally coordinated Al^{3+} site with trigonal distortion (though with Γ_3 as the lower level), Orbach broadening sets in abruptly above 35 K, and from its temperature dependence an energy difference $\Delta W = 258\ \mathrm{cm}^{-1}$ has been estimated,[28] however a linewidth of 10 mT corresponding to our case is attained only near the disappearance temperature ~ 45 K. In the similar Al_2O_3:Ti^{3+} case there is a smaller splitting $\Delta W = 38\ \mathrm{cm}^{-1}$, leading to broadening and disappearance of the signal already near 12 K.[3,29] Another example for Ti^{3+} with Orbach broadening is in yttrium aluminum perovskite,[30] where Ti^{3+} substitutes for an orthorhombic Al^{3+} site with $\Delta W = 170\ \mathrm{cm}^{-1}$ and $T_{dis} = 55$ K. These comparisons suggest that in our case the vibronic reduction derived using the first-order approximation is somewhat overestimated. Accordingly, there must be further reasons for the thermal behavior of the EPR intensity, required anyway by the rather unusual temperature dependence of the linewidth.

As shown previously[10] for Ti_{Li}^{3+} and Nb_{Li}^{4+}, the linewidth is partly due to inhomogeneous broadening resulting from a distribution of g values. Such a distribution is ultimately caused by the sensitivity of the centers to random elastic stresses in the crystal that is characteristic for ferroelectrics like $LiNbO_3$, especially in the presence of intrinsic defects and aliovalent dopants. It is a straightforward assumption to expect stronger sensitivity in the case of enhanced vibronic coupling that explains the larger linewidths observed at low temperatures for Nb substitution (compare the values for $T = 20$ K in Table I). The larger linewidths towards lower temperatures for Ti_{Nb}^{3+} are apparently interrelated to the steeper temperature dependence of the g values in this region (see Fig. 3). These low-temperature anomalies might be caused by small displacements of the equilibrium positions of the potential minima for the adiabatic potential and/or by a transition from the dynamic to the static JT effect. For higher temperatures motional effects may counteract broadening due to spin relaxation.[10] Motional narrowing may be related to spin-conserving intervalence transfer to lattice niobiums, which is another possible cause of partial thermal depopulation to be further discussed in the next section.

Concluding this section, we can only repeat the warning of the authors of Ref. 2 not to take the derived JT parameters at their face value. However, we believe our comparisons made for various centers and substitution sites to be qualitatively correct. As an independent approach for all four systems, simultaneous multiphonon calculations of the JT energies and the positions of the potential minima of the $T \times e$ adiabatic potential would be helpful.

B. Discussion of photoexcitation effects

The photoinduced effects observed by us for the Ti_{Nb}^{3+} and Nb_{Nb}^{4+} centers in $LiNbO_3$:Mg:Ti (Figs. 4 and 5) are very similar to those reported for the corresponding Li substituting centers in $LiNbO_3$:Ti,[1,2,8] and can be attributed to electron transfer from Ti^{3+} to Nb^{5+}, resulting in Ti^{4+} and Nb^{4+} centers. An important difference is the partial low-temperature recovery of the EPR signals seen after switching off the illumination (see Fig. 5) that was not reported for the

Li substituting centers. There is also a somewhat larger fraction of residual Ti^{3+} centers probably due to fast recombination during illumination. In our opinion these differences are due to smaller spatial distances between the $Ti^{4+/3+}$–$Nb^{5+/4+}$ pair constituents in the Nb substitution case. Some overlap of the involved potential wells and the respective electronic states may facilitate the reverse charge transfer without the participation of the conduction-band states.

Such a vicinity in our case may have the simple reason that the location of a Nb_{Nb}^{4+} center produced by illumination may be a more or less normal Nb site next to the given $Ti_{Nb}^{4+/3+}$ ion, while for the corresponding Li substitution case there is no reason to assume the presence of an antisite Nb_{Li} defect next to a Ti_{Li} center. An important role is played apparently by the distribution of the codopant Mg present in a surplus concentration in our samples. The presence of nearby Mg^{2+} ions was assumed earlier for the stabilization of intrinsic Nb_{Nb}^{4+} polarons[4–6] and O^- defects[31] in $LiNbO_3$:Mg. In our double-doped crystals at least part of the $Ti_{Nb}^{4+/3+}$ centers may be charge compensated by one or even two nearby Mg_{Li}^{2+} compensators. Such complexes are neutral either for the as-grown Ti_{Nb}^{4+} state (1 compensator) or for the reduced Ti_{Nb}^{3+} state (2 compensators) and singly charged in their other state. Illumination apparently results in a short distance electron transfer from the titanium to a niobium situated close to a charge compensator. Evidently, there may be a number of possible geometries for the involved Ti_{Nb}-Nb_{Nb}-Mg_{Li} and possible Ti_{Nb}-Nb_{Nb}-$(Mg_{Li})_2$ complexes, explaining their differing recovery properties, the slightly asymmetric EPR line shapes and the narrowing of the line upon illumination.

Part of the Ti^{3+} centers recovers in the dark on the minute scale with an extremely small activation energy of $\Delta E_d/k_B = (7 \pm 3)$ K, or even faster during illumination. These may be stable, well-compensated centers (possibly with a second nearby Mg^{2+}). Another part remains destroyed after low-temperature illumination and is apparently more weakly compensated. A further fraction, the fraction of uncompensated Ti^{4+} centers not responding to the reduction treatment can be assumed to be rather small due to the large number of available charge compensators in the crystal.

The large initial intensity of the Ti_{Nb}^{3+} signal compared to that of the Nb_{Nb}^{4+} signal and also the photoexcitation and recovery effects (see Figs. 1 and 5) are clear indications for the lower position of the $Ti_{Nb}^{4+/3+}$ energetic level compared to $Nb_{Nb}^{5+/4+}$. This is similar to the situation found for the corresponding centers on Li site having levels near the conduction band edge.[1,2,8] In our case apparently both levels are even closer to the band edge. The $Nb_{Li}^{5+/4+}$ level is expected to be deeper than the $Nb_{Nb}^{5+/4+}$ polaron level formed essentially from Nb $4d$ states of the conduction band,[8] even if a substantial part of the difference may be made off by interaction with nearby defects.

The average energy difference ΔE between the $Ti_{Nb}^{4+/3+}$ and $Nb_{Nb}^{5+/4+}$ levels participating in the charge-transfer processes can be derived by estimating concentration data for a temperature where the system is in thermal equilibrium, i.e., the concentrations are independent both of previous illumination treatments and the way of reaching this temperature. Such a temperature may be the recovery temperature 105 ± 15 K after photoexcitation. From the mass action law, we have for the equilibrium center concentrations

$$\frac{[Ti_{Nb}^{4+}] \times [Nb_{Nb}^{4+}]}{[Ti_{Nb}^{3+}] \times [Nb_{Nb}^{5+}]} = e^{-\Delta E/k_B T}, \tag{7}$$

as there is no entropy change for charge transfer between states of identical degeneracy. The $[Nb_{Nb}^{4+}]/[Ti_{Nb}^{3+}]$ ratio can be estimated as the ratio of integral intensities of the EPR signals, but only at lower temperatures. Still, we can derive lower and upper limits for the equilibrium ratio valid at 105 K: by quenching the crystal from the recovery temperature and measuring at $T = 14$ K, we obtain a lower limit, while measuring the ratio at $T = 74$ K during the thermal recovery process in a crystal previously illuminated at low temperatures we get an upper limit of the ratio. The corresponding experimental results are 0.55 and 0.74. For an upper limit of $[Ti_{Nb}^{4+}]$, we take the upper limit of the total titanium concentration incorporated into the crystal $[Ti]_{max} = 0.08$ mol %. For a lower limit of $[Ti_{Nb}^{4+}]$, we take the difference $[Ti]_{min} - [Ti^{3+}]_{max}$. Here $[Ti]_{min} = 0.04$ mol %, and the maximal Ti^{3+} concentration reconcilable with low-temperature EPR measurements is 0.016 mol %, so we have 0.024 mol % as a lower limit of $[Ti_{Nb}^{4+}]$. For $[Nb_{Nb}^{5+}]$, which should be in our case the concentration of lattice niobiums capable to trap and stabilize an electron, we may choose values between 24 and 100 mol % corresponding to only three nearest Nb sites for each Mg compensator or all Nb sites, respectively, as we do not know how far the charge compensator has to be. Taking into account these uncertainties we obtain the average $\Delta E = 70 \pm 23$ meV, which is smaller or comparable than the value $\Delta E = 110 \pm 20$ meV reported[2] for the energy difference of the respective levels of the same ions on Li sites. This indicates that in the Nb substitution case also, the average $Ti^{4+/3+}$ level is closer to the band edge than for Li substitution.

However, the above average neglects the interactions within the Ti-Nb-Mg_n complexes (where n is a small integer) present in appreciable though relatively small numbers compared to the values taken for $[Nb_{Nb}^{5+}]$. For charge transfer within such complexes, the energetic difference may be even smaller than the above value. This provides an effective mechanism for appreciable thermal depopulation of the Ti^{3+} ground state, explaining the observed steeper than Curie-like temperature dependence of the EPR intensity, without assuming thermal excitation within the Ti^{3+} ion.

As shown by the slightly different ratio of intensity changes during photoexcitation and partial recovery (see Fig. 5), the presence of other traps than Ti and Nb centers cannot be fully excluded in our reduced crystals, though such centers could not be identified. The presence of other identified electron traps, i.e., OH^- centers have been the cause of the failure of producing Ti^{3+} centers by low-temperature γ irradiation in as-grown $LiNbO_3$:Mg:Ti crystals.[6] These ions have deep $OH^{1-/2-}$ donor levels in the gap that are more efficient electron traps than Ti^{4+} and Nb^{5+}. In fact, in $LiNbO_3$:Mg:Ti, similarly to $LiNbO_3$:Mg crystals,[32,31] γ irradiation produces only OH^{2-} trapped electron centers along with O^-(Mg) trapped-hole centers. During high-temperature

vacuum reduction there is an outdiffusion of hydrogen from the crystal with a simultaneous rise of the Fermi level resulting in the formation of only Ti_{Nb}^{3+} and Nb_{Nb}^{4+} centers.

V. CONCLUSION

We reported on the creation of an axial paramagnetic center in vacuum annealed $LiNbO_3$:Mg:Ti and described it as a Ti^{3+} ion on a Nb site. The unprecedentedly low value of the orbital reduction factor and the unusual $g_{\|} \leqslant g_{\perp}$ relation obtained cannot be explained by usual covalency effects and require additional strong vibronic coupling leading to a dynamic pseudo-Jahn-Teller effect. The results indicate a nearly isotropic center with a nearly degenerate ground state where the JT coupling becomes a large interaction among those relevant for the ground state. Comparing the results with literature data on other Ti^{3+} and Nb^{4+} centers on octahedrally coordinated sites in $LiNbO_3$, we find the vibronic coupling to be stronger for Ti^{3+} than for Nb^{4+}, and stronger for the Nb than for the Li substitution site. The strength of the coupling appears to be anticorrelated to the positive charge misfit. The qualitative difference between the estimated value of the trigonal ground-state splitting of a given ion on the Nb site and the respective value for the Li substitution site can be understood as resulting from structural constraints: ions substituted for Li are confined to more displaced sites than those on Nb sites. The data and the established trends have been used for the tentative prediction of thermal displacements of Nb^{4+} ions away from the octahedron center.

Using low-temperature photoexcitation we showed that unpaired electrons on the Ti^{3+} centers can be transferred to the matrix forming Nb^{4+} centers on Nb sites. The observed recombination effects, partly at low temperature in the dark and the rest upon annealing, indicate the existence of slightly different Ti^{3+} centers as suggested also by line shape properties. The findings can be explained by the existence of Ti-Mg and possibly also Mg-Ti-Mg complexes with various interatomic distances. Mg^{2+} ions on Li sites apparently play the role of charge compensators for both the Ti_{Nb}^{3+} and the Nb_{Nb}^{4+} centers. The average energetic difference between these two types of donor states is estimated to be smaller than for the respective Li substituting centers in the absence of Mg.

ACKNOWLEDGMENTS

The authors are indebted to Professor Schirmer and Professor A. B. Roitsin for useful discussions and important remarks concerning the topic, and to Dr. Malovichko and S. P. Kolesnik for technical help. Support of the ESF Oxide Crystal Network, and grants of the Hungarian Science and Research Fund (T24092, T23092, and F24088) are kindly acknowledged.

*Electronic address: corradi@power.szfki.kfki.hu

†Present address: VEECO Instruments, 1 Terminal Drive, Plainview, NY 11803.

[1] S. Juppe and O. F. Schirmer, Phys. Lett. A **117**, 150 (1986).

[2] O. Thiemann, H. Donnerberg, M. Wöhlecke, and O. F. Schirmer, Phys. Rev. B **49**, 5845 (1994).

[3] R. M. Macfarlane, J. Y. Wong, and M. D. Sturge, Phys. Rev. **166**, 250 (1968).

[4] K. L. Sweeney, L. E. Halliburton, D. A. Bryan, R. R. Rice, R. Gerson, and H. E. Tomaschke, J. Appl. Phys. **57**, 1036 (1985).

[5] B. Faust, H. Müller, and O. F. Schirmer, Ferroelectrics **153**, 297 (1994); see also B. Faust, Diplomarbeit, Osnabrück University, 1992.

[6] I. M. Zaritskii, L. G. Rakitina, and K. Polgár, Fiz. Tverd. Tela **37**, 1970 (1995) [Phys. Solid State **37**, 1073 (1995)].

[7] O. F. Schirmer and D. von der Linde, Appl. Phys. Lett. **33**, 35 (1978).

[8] O. F. Schirmer, O. Thiemann, and M. Wöhlecke, J. Phys. Chem. Solids **52**, 185 (1991).

[9] G. Corradi, K. Polgár, I. M. Zaritskii, L. G. Rakitina, and N. I. Deryugina, Fiz. Tverd. Tela **31**, 115 (1989) [Sov. Phys. Solid State **31**, 1540 (1989)].

[10] L. G. Rakitina, I. M. Zaritskii, G. Corradi, and K. Polgár, Fiz. Tverd. Tela **32**, 1112 (1990) [Sov. Phys. Solid State **32**, 652 (1990)].

[11] L. Malicskó, I. Cravero, and Th. Krajewski, Cryst. Res. Technol. **19**, 999 (1984).

[12] A. Räuber, in *Current Topics in Materials Science*, edited by E. Kaldis (North-Holland, Amsterdam, 1978), Vol. 1, p. 481.

[13] L. Kovács, G. Ruschhaupt, K. Polgár, G. Corradi, and M. Wöhlecke, Appl. Phys. Lett. **70**, 2801 (1997).

[14] A. Abragam and B. Bleaney, *Electron Paramagnetic Resonance of Transition Ions* (Clarendon, Oxford, 1970).

[15] C. Zaldo, C. Prieto, H. Dexpert, and P. Fessler, J. Phys.: Condens. Matter **3**, 4135 (1991).

[16] L. Rebouta, M. F. da Silva, J. C. Soares, J. A. Sanz-Garcia, E. Diéguez, and F. Agulló-López, Nucl. Instrum. Methods Phys. Res. B **64**, 189 (1992).

[17] B. Hauer, R. Vianden, M. F. da Silva, L. Rebouta, J. C. Soares, E. Diéguez, and F. Agulló-López, J. Phys.: Condens. Matter **6**, 267 (1994).

[18] H. Donnerberg, S. M. Tomlinson, C. R. A. Catlow, and O. F. Schirmer, Phys. Rev. B **44**, 4877 (1991).

[19] C. Prieto and C. Zaldo, J. Phys.: Condens. Matter **6**, L677 (1994).

[20] J. G. Marques, C. M. de Jesus, A. A. Melo, J. C. Soares, E. Diéguez, and F. Agulló-López, in *Proceedings of the 10th International Conference on Hyperfine Interactions*, Leuven, 1995, edited by M. Rots *et al.* [Hyperfine Interact. **1**, 348 (1996)].

[21] G. Corradi, H. Söthe, J.-M. Spaeth, and K. Polgár, J. Phys.: Condens. Matter **3**, 1901 (1991).

[22] G. Corradi, A. V. Chadwick, A. R. West, K. Cruickshank, and M. Paul, Radiat. Eff. Defects Solids **134**, 219 (1995).

[23] J. Diaz-Caro, J. Garcia-Solé, D. Bravo, J. A. Sanz-Garcia, F. J. Lopez, and F. Jaque, Phys. Rev. B **54**, 13 042 (1996).

[24] F. Huixian, W. Jinke, W. Huafu, H. Shiying, and X. Yunxia, J. Phys. Chem. Solids **51**, 397 (1990).

[25] A. Böker, H. Donnerberg, O. F. Schirmer, and F. Xiqi, J. Phys.: Condens. Matter **2**, 6865 (1990).

[26] C. A. Bates and J. P. Bentley, J. Phys. C **2**, 1947 (1969).

[27] G. Corradi, K. Polgár, A. A. Bugaii, I. M. Zaritskii, L. G. Rakitina, V. G. Grachev, and N. I. Derjugina, Fiz. Tverd. Tela **28**, 739 (1986) [Sov. Phys. Solid State **28**, 412 (1986)].

[28] G. Wang, H. G. Gallagher, T. P. J. Han, B. Henderson, M. Yamaga, and T. Yoshida, J. Phys.: Condens. Matter **9**, 1649 (1997).

[29] N. E. Kask, L. S. Kornienko, T. S. Mandel'shtam, and A. M. Prohorov, Fiz. Tverd. Tela **5**, 2306 (1963) [Sov. Phys. Solid State **5**, 1677 (1964)].

[30] M. Yamaga, T. Yoshida, B. Henderson, K. P. O'Donnell, and M. Date, J. Phys.: Condens. Matter **4**, 7285 (1992).

[31] I. M. Zaritskii, L. G. Rakitina, G. Corradi, K. Polgár, and A. A. Bugai, J. Phys.: Condens. Matter **3**, 8457 (1991).

[32] L. G. Rakitina, I. M. Zaritskii, and K. Polgár, Appl. Magn. Reson. **1**, 149 (1990).